Received: 31 August 2020 | Revised: 3 December 2020 | Accepted: 3 December 2020

DOI: 10.1111/pce.13977

ORIGINAL ARTICLE

Plant, Cell & Environment WILEY

Modelling the physiological relevance of sucrose export repression by an Flowering Time homolog in the long-distance phloem of potato

Bas van den Herik[1] | Sara Bergonzi[2] | Christian W. B. Bachem[2] | Kirsten ten Tusscher[1]

[1]Computational Developmental Biology, Utrecht University, Utrecht, The Netherlands

[2]Plant Breeding, Wageningen University & Research, Wageningen, The Netherlands

Correspondence
Kirsten ten Tusscher, Computational Developmental Biology Group, Department of Biology, Faculty of Science, Utrecht University, Padualaan 8, 3584 CH Utrecht, The Netherlands.

Abstract

Yield of harvestable plant organs depends on photosynthetic assimilate production in source leaves, long-distance sucrose transport and sink-strength. While photosynthesis optimization has received considerable interest for optimizing plant yield, the potential for improving long-distance sucrose transport has received far less attention. Interestingly, a recent potato study demonstrates that the tuberigen StSP6A binds to and reduces activity of the StSWEET11 sucrose exporter. While the study suggested that reducing phloem sucrose efflux may enhance tuber yield, the precise mechanism and physiological relevance of this effect remained an open question. Here, we develop the first mechanistic model for sucrose transport, parameterized for potato plants. The model incorporates SWEET-mediated sucrose export, SUT-mediated sucrose retrieval from the apoplast and StSP6A-StSWEET11 interactions. Using this model, we were able to substantiate the physiological relevance of the StSP6A-StSWEET11 interaction in the long-distance phloem for potato tuber yield, as well as to show the non-linear nature of this effect.

KEYWORDS

efflux-retrieval, phloem, *Solanum tuberosum*, StSP6A, StSWEET11, transport

1 | INTRODUCTION

Sucrose availability is a major determinant of plant organ growth and hence yield of harvestable crop organs, such as fruits, seeds, roots and tubers. Therefore, considerable research effort has been and is directed towards optimizing photosynthesis efficiency, and this has led to spectacular yield improvements in some crop species (Driever et al., 2017; Nölke, Houdelet, Kreuzaler, Peterhänsel, & Schillberg, 2014). However, plant growth and yield ultimately depend on the amount of sucrose delivered to sink organs per unit of time. Photosynthate availability in source-leaves is thus not the only factor-influencing yield, and long-distance transport, sink unloading mechanism and sink-strength also impact the final crop yield (Fernie et al., 2020). Indeed, it has been previously shown that coordinated regulation of source and sink strengths has a major impact on plant yield (Jonik, Sonnewald, Hajirezaei, Flügge, & Ludewig, 2012).

Predicting the effect of photosynthate availability, sink-strength and long-distance phloem transport characteristics on plant yield is far from trivial. Similar sized improvements in photosynthesis efficiency may have variable effects on yield in different species due to different feedback regulations or differences in limiting factors (Fernie et al., 2020). Furthermore, sucrose transport is a highly complex,

multi-feedback biophysical process, with source- and sink-strengths affecting phloem sucrose concentration gradients, which in turn, affect phloem sap viscosity and pressure gradients, with these also determining phloem flow velocity, and providing feedback into the sucrose concentration gradients. Although the xylem-mediated upward transport of water and mineral nutrients occurs through a distinct, transpiration induced pressure gradient, phloem and xylem water flows are hydraulically coupled, giving rise to additional feedbacks on phloem transport. Due to these complexities, mathematical modelling is an invaluable tool to unravel the effects of various aspects of sucrose transport on plant yield (De Schepper & Steppe, 2010; Hölttä, Vesala, Sevanto, Perämäki, & Nikinmaa, 2006; Lacointe & Minchin, 2008; Sellier & Mammeri, 2019; Sevanto, Hölttä, & Holbrook, 2011). So far mathematical models have primarily been restricted to large plants and trees (>5 m stem, Table S1). A first major goal of this study is therefore to develop a quantitative model for sucrose transport for an agronomically relevant crop species, potato, with source-sink distances of maximum 1.5 m.

In addition to the long-distance convective transport of sucrose through the phloem from source to sink tissues, an exchange of sucrose between the phloem and the surrounding tissues also takes place. Export of phloem sucrose into the apoplast is mediated by so-called SWEET transporters, which facilitate gradient-dependent bidirectional transport (Chen et al., 2012). Therefore, SWEET-mediated sucrose transport depends on phloem and apoplast sucrose levels. Besides SWEETs, the SUT/SUC sucrose importers are expressed in the phloem (Hafke et al., 2005). These importers enable sucrose retrieval from the apoplast, thereby reducing net phloem sucrose loss (Minchin & Lacointe, 2017). Interestingly, in a recent study, we showed that in heterologous expression experiments StSWEET11, an important potato phloem sucrose exporter, is bound by StSP6A, resulting in an approximately 40% reduction of its sucrose transport capacity (Abelenda et al., 2019). StSP6A is the tuberigen known to induce the developmental transition to tuber formation and enhancement of potato yield in greenhouse pot experiments (Navarro et al., 2011). These results suggest that, in addition to their potential role in the switch from apoplastic to symplastic unloading in the stolon (Abelenda et al., 2019), the StSP6A-StSWEET11 interaction increases yield by reducing sucrose efflux from the long-distance transport phloem. Although representing a plausible scenario, data from a transcriptomics analysis indicate that StSP6A also has a substantial effect on the expression of many other genes (Navarro et al., 2011). Thus, the observed StSP6A-mediated enhancement of potato yield may not necessarily or solely arise from StSP6A induced reduction of StSWEET11 sucrose transport. Experimentally, these different contributions of StSP6A to yield improvement are not easy to tease apart. Moreover, quantifying SWEET sucrose export and StSP6A-mediated reductions therein is difficult *in planta*. Therefore, a second major goal of this study is to use our model to study the potential physiological relevance of StSP6A-mediated reduction of StSWEET11 sucrose export on potato yield.

To this end, we here develop the first quantitative, mechanistic model for sucrose transport in the stem of potato plants. The model is based on the well-established phloem and xylem transport models by Hölttä et al. (2006), Lacointe and Minchin (2008) and Thompson and Holbrook (2003) that we have fully re-parameterized to potato-specific conditions. Using our model, we find that in potato, sucrose transport is dictated by viscous forces rather than sieve tube geometry. Next, we incorporated SWEET-mediated sucrose efflux, enabling us to estimate *in planta* SWEET transport rates necessary to reproduce physiologically relevant sucrose efflux, a value that cannot be easily extrapolated from available heterologous expression experimental data. Subsequently, we extended the model with SUT-mediated sucrose retrieval. To arrive at realistic temporal dynamics for phloem and apoplast sucrose levels, we improved upon existing models incorporating efflux and retrieval dynamics (Cabrita, Thorpe, & Huber, 2013; Minchin & Lacointe, 2017), incorporating realistic apoplast volumes as well as apoplast sucrose export to neighbouring tissues. As a final step, we incorporated the StSP6A-mediated 40% reduction of StSWEET11-mediated sucrose export. Our model confirms the physiological significance of StSP6A-mediated StSWEET11 blockage when physiologically relevant StSWEET11 transport rates are assumed. Furthermore, we find that, as a result of the non-linearities and feedbacks present in sucrose transport a 40% reduction in StSWEET11-mediated-efflux results in a greater increase in sucrose retention, that is, a larger than 40% reduction of yield loss.

2 | METHODS

We here provide a concise description of the model structure, assumptions, equations and implementation. A more detailed version of the methods is provided in the supplementary materials.

2.1 | Model structure and main assumptions

We used the well-established model for phloem transport by Thompson and Holbrook (2003) and coupled phloem-xylem transport (Hölttä et al., 2006; Lacointe & Minchin, 2008) as a starting point (Table S1). Our model includes phloem (Ph), xylem (X) and apoplast (A) longitudinal compartments. Within these compartments, three variables were defined, water mass (W) in g, pressure (P) in MPa, and sucrose (S) in mol. Compartment volume (V) and sucrose concentration (C) were derived from the water mass and sucrose amount (Table 1). The stem was divided into three zones; loading zone, unloading zone, and long-distance pathway (Van Bel, 2003), and discretized into N, cylindrical, elements (Figure 1a). The location (along the stem) and compartment type (phloem, xylem, apoplast) of the variables are notated using subscripts: $Var_{comp,j}$ in which comp represents the compartment and j the element position.

The model explicitly describes water and solute flow in the phloem, water flow in the xylem, SWEET and SUT-mediated sucrose exchange between the phloem and the apoplast, and water exchange between the xylem and phloem. Water flow in the xylem is driven by water transpiration in the topmost element as described by the cohesion-tension theory, while phloem water flow is driven by a

TABLE 1 Symbols and units for the used variables in the model

Variable	Symbol	Units
Water mass	W	g
Sucrose	S	mol
Pressure	P	MPa
Volume	V	m^3
Sucrose concentration	C	mol/m^3
Axial water flow	$J_{W,ax,in/out,Ph/X,j}$	g/s
Axial sucrose flow	$J_{S,ax,in/out,Ph/X,j}$	mol/s
Radial water flow	$J_{W,rad,in/out,Ph/X,j}$	g/s
Radial sucrose flow	$J_{S,rad,in/out,Ph/X,j}$	mol/s
Water potential	$\Psi_{Ph/X,j}$	MPa
Axial area	$A_{Ph/X,j}$	m^2
Radial area	$A_{rad,j}$	m^2
Osmotic potential	$\Pi_{X,j}$	MPa
Dynamic viscosity	$\mu_{Ph,j}$	MPa/s
Sucrose loading	$L_{Ph,j}$	mol/s
Sucrose unloading	$U_{Ph,j}$	mol/s
Sucrose efflux/retrieval	$E_{Ph,j}$	mol/s

hydrostatic pressure gradient induced by sucrose loading and unloading as described by the Münch-hypothesis. Water exchange between phloem and xylem is modelled in a simplified manner as a water potential driven water flux over a semi-permeable membrane (Equation (3)), without describing the details of symplastic and apoplastic transport components. Inherent to this simplified description in which water dynamics in the apoplast are ignored is the assumption that apoplastic water volume stays constant (implying non-growth conditions), and that no axial flow occurs in the apoplastic space. Importantly, this axial apoplastic water flow is considered far less efficient than phloem bulk flow, making this an acceptable approximation. Radial transport of sucrose from the phloem and apoplast to the xylem is also ignored as limited data are available on the active sucrose uptake by tissues neighbouring and symplastically connected to the xylem. Available data suggest that imported sucrose serves to fuel secondary cell wall thickening and other local processes rather than long-distance xylem transport (Aubry, Dinant, Vilaine, Bellini, & Le Hir, 2019). This results in relatively minor xylem sucrose levels that can be ignored for the purposes of this study, as has been done in previous modelling work (de Schepper & Steppe, 2010; Hölttä et al., 2006). These assumptions are further supported by the low

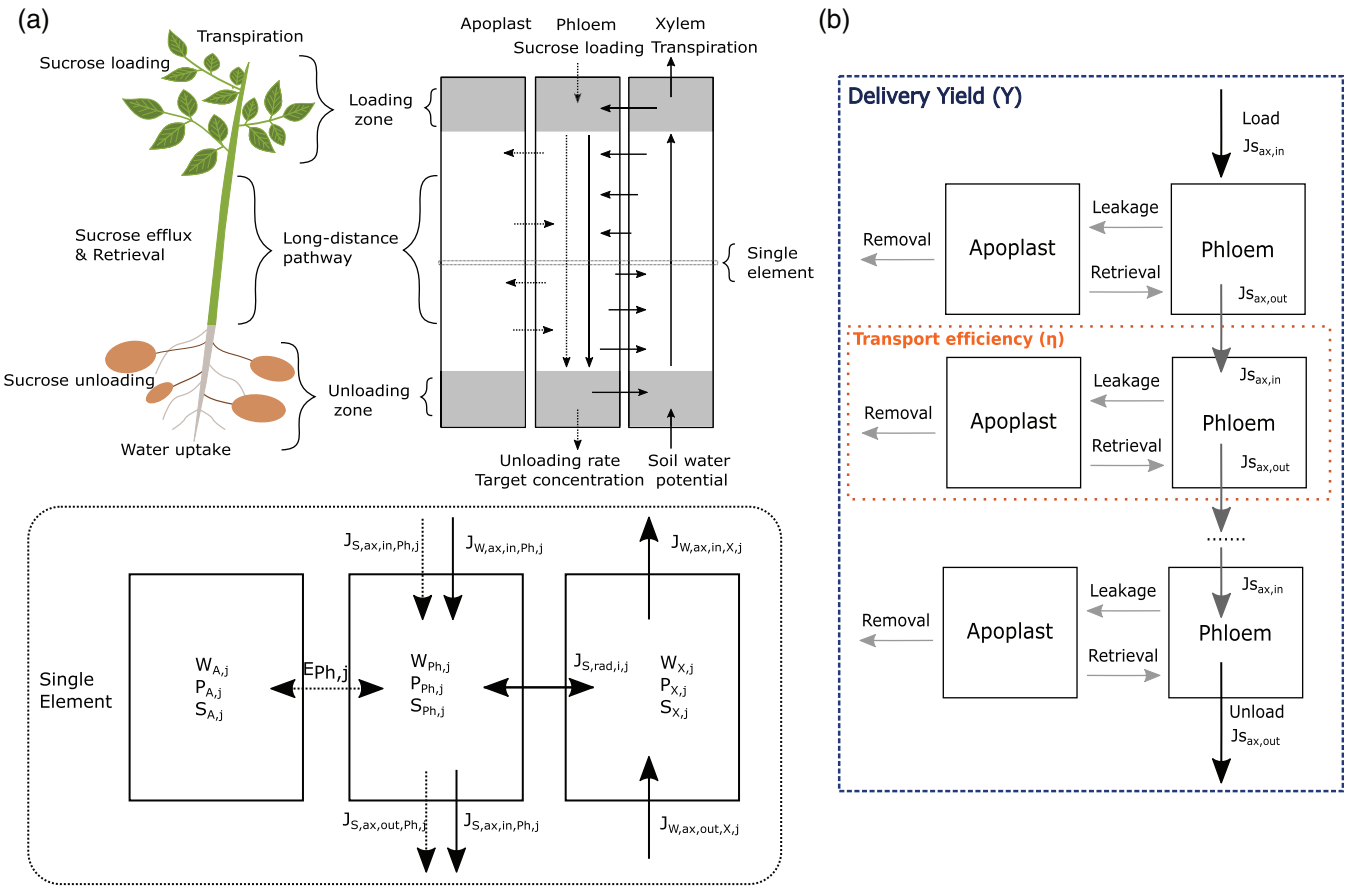

FIGURE 1 Overview of the model architecture, processes and yield/efficiency. (a) Modelled processes and localization in the plant are depicted left, A schematic, longitudinal model overview with the loading and unloading zones indicated in grey is shown on the right, water flow is depicted with solid arrows and sucrose flow with dotted arrows. The xylem and phloem boundary conditions at the top and bottom are shown. On the bottom, a zoom-in on a single element, consisting of neighbouring phloem, xylem and apoplast compartments. Depicted are the in- and outflow of water and sucrose as well as the variables included in a single element (j). (b) Transport efficiency and delivery yield (Equations (14) and (15)). Delivery yield is calculated over the complete system (dashed line), whereas the transport efficiency is calculated per element (dotted line)

concentrations of sucrose in xylem fluid measurements (Pagliarani et al., 2019; Secchi & Zwieniecki, 2016). Further, we did not include the potential presence of a radial sucrose gradient in the apoplastic compartment as assuming a gradient would enhance sucrose levels next to the phloem while decreasing from sucrose levels away from the phloem. Consequently, sucrose retrieval efficiency from the apoplast to the phloem would be enhanced due to a gradient, and our simulations represent a worst-case scenario.

2.2 | Model equations

2.2.1 | Water and pressure

Water transport in the stem is described using the following system of equations:

$$\frac{\partial W_{Ph/X,j}}{\partial t} = \left(J_{W,ax,in,Ph/X,j} - J_{W,ax,out,Ph/X,j} + J_{W,rad,in,Ph/X,j} - J_{W,rad,out,Ph/X,j}\right)\rho \quad (1)$$

$$J_{W,Ph/X,j,ax} = A_{i,j}\frac{k_{i,j}}{\mu_{i,j}}\frac{\partial P_{Ph/X,j}}{\partial x} = A_{Ph/X,j}\frac{k_{Ph/X,j}}{\mu_{Ph/X,j}}\frac{P_{Ph/X,j-1} - P_{Ph/X,j}}{x} \quad (2)$$

$$J_{W,rad,in,Ph,j} = L_r A_{rad,j}\left(\Psi_{X,j} - \Psi_{Ph,j}\right) \quad (3)$$

$$\Pi_{Ph,j} = -\rho RT\left(0.998m_{Ph,j} + 0.089m_{Ph,j}^2\right) \text{ with } m_{Ph,j} = \frac{C_{Ph,j}}{\rho\left(1 - C_{Ph,j}V_{suc}\right)} \quad (4)$$

(Michel, 1972)

$$\mu_{Ph,j} = \mu_X exp\left(\frac{4.68 * 0.956\phi_{Ph,j,}}{1 - 0.956\phi_{Ph,j}}\right) \text{ with } \phi_{Ph,j} = \frac{V_{suc}S_{Ph,i}}{V_{suc}S_{Ph,i} + V_{Ph,i}} \quad (5)$$

(Morison, 2002)

$$\frac{\partial P_{Ph/X,j}}{\partial t} = \varepsilon_{Ph/X,j}\frac{1}{W_{Ph/X,j}}\frac{\partial W_{Ph/X,j}}{\partial t} \quad (6)$$

$$A_{Ph,j} = A_0 e^{\frac{\left(P_{Ph,j} - P_0\right)}{\varepsilon_{Ph,j}}} \quad (7)$$

(Thompson & Holbrook, 2003)with $J_{W,ax,in,Ph/X,j}$ axial water inflow and $J_{W,rad,in,Ph/X,j}$ radial water inflow, $\psi_{Ph/X,j}$ water potential, $\Pi_{Ph,j}$ phloem osmotic potential, $\mu_{Ph,j}$ phloem sap viscosity and $A_{Ph/X,j}$ axial area. All variables are defined in Table 1, while parameters are described in Table 2. The axial outflow rate is set equal to the inflow rate of the element below, similarly the radial inflow rate in the phloem is set equal to the outflow rate of the xylem. As boundary conditions in the phloem, we set the respective inflow and outflow equal to zero. For the boundaries in the xylem, we applied measured water transpiration and soil water potential.

2.2.2 | Sucrose

Sucrose transport is described using the following set of equations:

$$\frac{\partial S_{Ph,j}}{\partial t} = J_{S,ax,in,Ph,j} - J_{S,ax,out,Ph,j} - J_{S,Rad,Ph,j} \quad (8)$$

$$J_{S,ax,in,Ph,j} = J_{W,ax,in,Ph,j} \times C_{Ph,j-1} \quad (9)$$

$$J_{S,rad,Ph,j} = L_{Ph,j} - U_{Ph,j} - E_{Ph,j} \quad (10)$$

$$U_{Ph,j} = v_{unload} \times \left(C_{Ph,j} - C_{target}\right) \quad (11)$$

$$E_{Ph,j} = v_{MaxSWEET}V_{Ph,j}\frac{C_{Ph,j}}{C_{Ph,j} + K_{mIn}} - v_{MaxSWEET}V_{Ph,j}\frac{C_{A,j}}{C_{A,j} + K_{mEx}} - v_{MaxSUC}V_{Ph,j}\frac{C_{A,j}}{C_{A,j} + K_{mSUC}} \quad (12)$$

$$\frac{dS_{A,j}}{dt} = E_{Ph,j} - v_{resp}\frac{C_{A,j}}{C_{A,j} + K_{mR}} \quad (13)$$

With $J_{S,ax,in,Ph,j}$ axial sucrose inflow, sucrose outflow is set equal to sucrose inflow of the element below, equal to the approach taken for water flow. $J_{S,rad,Ph,j}$ radial sucrose transport, consisting of a constant uptake at the loading zone ($L_{Ph,j}$), concentration dependent loss at the unloading zone ($U_{Ph,j}$) and SWEET-mediated bi-directional exchange with- and SUC-mediated retrieval from the apoplast along the long-distance pathway ($E_{Ph,j}$). We observed that increasing loading rate, that is, increasing photosynthetic efficiency, enhances sucrose delivery (Figure S1). For loading rates beyond a factor 2.5× the standard loading rate, a viscosity induced increase in resistance resulted in non-physiologically realistic high sucrose concentrations, pressure and flow velocities. *In planta*, this regime is likely prevented by feedback regulation on sucrose import, photosynthesis and sink strength, absent in our current model. Further note that through maintaining a constant target tuber concentration (C_{target}) and employing a high unloading rate (v_{unload}), our model system is in a non-sink-limited regime (Figure S1). This enables us to focus on the impact of changes in long-distance phloem transport on tuber sucrose delivery.

2.2.3 | Defining transport efficiency and delivery yield

Since we are interested in the effects of efflux and retrieval on potato tuber formation, we define two quantification measures (Figure 1b). To quantify the effect of sucrose efflux and retrieval along the stem, we introduce the measure of transport efficiency (η). We define it as the ratio of sucrose output over sucrose input per element, which for steady-state simplifies to the ratio of axial outflow over inflow:

TABLE 2 Parameters for the Thompson and Holbrook (2003) and the potato-specific model

Parameter	Symbol	Thompson and Holbrook	Potato	Units	References potato parameters
Density of water	ρ	0.998e6		g/m^3	-
Partial molal volume sucrose	V_{suc}	0.2155e-3		m^3/mol	-
Gas constant	R	8.314e-6		MPa m^3 /K/mol	-
Temperature	T	293		K	-
Radial hydraulic membrane permeability	L_r	5e-8		m/Mpa/s	-
Dynamic viscosity water/ xylem	μ_x	1.0019e-9		MPa/s	-
Stem length	l	5	1	m	Vos and van der Putten (1998)
Phloem sieve element radius	r_p	7.5e-6 at t = 0	8.4e-6 (10.7e-6 before tuning) at t = 0,	m	Based on Mullendore, Windt, Van As, and Knoblauch (2010) and Aliche et al. (2020)
Xylem conduit radius	r_x	-	30e-6	m	Aliche et al. (2020)
Axial permeability phloem	k_p	0.928e-12	3.82e-12	m^2	Mullendore et al. (2010)
Elastic modulus phloem	ε_p	17	30	MPa	Nobel (2005)
Elastic modulus xylem	ε_x	-	750	MPa	Irvine and Grace (1997)
Transpiration rate	J_{trans}	-	0.02	g/s	Schans and Arntzen (1991)
Water potential soil	ψ_{soil}	-	0	MPa	Perämäki et al. (2001)
Sucrose loading rate	v_{load}	7.95e-11 (mol m^{-1} s^{-1})	1e-8 (mol/s)	-	Derived from: Pourazari, Andersson, and Weih (2018) Zeeman, Kossmann, and Smith (2010) Zheng et al. (2016)
Unloading rate	v_{unload}	v_load (mol m^{-1} s^{-1})	0.5e-10 (m^3/s)	-	-
Boundary concentration unloading zone	C^{target}	500	50	mol/m^3	Derived from: Bethke, Sabba, and Bussan (2009) Duarte-Delgado et al. (2016) Leggewie et al. (2003) Ross and Davies (1992)
Number of phloem sieve elements	E_{phloem}	-	100	-	Derived from: Aliche et al. (2020) Hölttä, Mencuccini, and Nikinmaa (2009) Sibout, Plantegenet, and Hardtke (2008)
Number of xylem conduits	E_{xylem}	-	150	-	Aliche et al. (2020)
Max. apoplast removal rate	R_{max}	-	0.4e-8	mol/s	Estimated
Affinity constant removal	$K_{m,R}$	-	5	mol/m^3	Estimated

$$\eta = \frac{outflow}{inflow} = \frac{J_{S,ax,out,Ph,j}}{J_{S,ax,in,Ph,j}} \quad (14)$$

A 100% transport efficiency implies that all sucrose received from a shootward-oriented phloem element is passed on by the current element to its rootward element, lower transport efficiencies indicate sucrose loss. To measure the effective supply of sucrose to the tubers and compare between different simulations, we introduce the measure of delivery yield (Y), which we define as the ratio of the amount of sucrose unloaded over the amount loaded in a given time interval (ranging from t_0 to t_{end}, by default over a 24 hr period starting after steady-state was reached):

$$Y = \frac{\sum_{j=1}^{N} \int_{t_0}^{t_{end}} \left(U_{Ph,j}\right)}{\sum_{j=1}^{N} \int_{t_0}^{t_{end}} \left(L_{Ph,j}\right)} \quad (15)$$

2.3 | Model parameters, implementation and simulations

An extensive description of how parameter values were derived can be found in the supplemental methods. The system of differential equations was implemented in MatlabR2019b and was solved using the build-in solver ode15s, using an integration time step of $\Delta t = 1$ s.

All simulations were started from zero initial pressure and sucrose. The initial element water mass was calculated from the model dimensions, resulting in an initial water mass per element of 5.9e-4g in the phloem loading/unloading zones, 1.1e-4g in the phloem long-distance zone, 2.1e-3g in the xylem loading/unloading zones and 1.1e-2g in the xylem long distance zone. The modelled plant stem was spatially discretized using a non-homogeneous mesh with 20 elements with a fine-grained spatial resolution of x = 0.005 m in the loading and unloading zone and 30 elements with a coarse-grained spatial resolution of x = 0.0267 m in the long-distance pathway. The non-homogeneous discretization mesh allowed for a reduction in the number of elements used in the long-distance zone without sacrificing resolution in the loading and unloading zones where high precision is needed due to steep gradients in sucrose as a result of sucrose loading and unloading and resulting enhanced lateral water fluxes. This approach reduced simulation time without significantly affecting model outcomes (Figure S2). The source code used for model simulations is available on: http://www-binf.bio.uu.nl/khwjtuss/PotatoSucroseTransport.

3 | RESULTS

3.1 | A baseline potato-specific transport model

To test the validity of the developed model, we benchmarked it against the main results from Thompson and Holbrook (2003) using identical parameter settings (Table 2). Model outcomes are quantitatively highly similar (Figure S3, Table S2), the observed small differences may arise from differences in model implementation details (e.g., used numerical solver) as earlier discussed by Mammeri and Sellier (2017). Adding a non-zero xylem potential resulted in decreased phloem volume (2.1%) and water flow (6.4%), increased sucrose concentration (6.9%) and a small decrease in pressure gradient (−0.5%) (Figure S3, Table S2), consistent with earlier work (De Schepper & Steppe, 2010; Hölttä et al., 2006; Sevanto et al., 2011). Further, when simulating nighttime (switching off transpiration), Münch-counterflow equal to phloem flow was observed in the xylem, as observed earlier (De Schepper & Steppe, 2010; Hölttä et al., 2006).

After this validation, we transformed the model to potato specific parameters, assuming a stem-length of 1 m, with loading and unloading zones of 0.1 m. We incorporated plant architectural and mechanical data on stem length, phloem and xylem characteristics (conduit radius, abundance and resistance, elastic modulus). Parameter values are provided in Table 2 and their detailed derivation in the supplementary methods section. Changing the stem length within the expected variation, for example, 0.5–1.5 m, did not qualitatively alter the outcomes and only had a minor impact on the transport characteristics (Figure S4). An important difference between potato and previously modelled plants was the higher axial permeability in the phloem, which results from differences in sieve-element and sieve-plate architecture (Mullendore et al., 2010). We derived a potato-specific lower limit for the phloem sucrose loading rate of 1e-8 mol/s, which is of the same order of magnitude as values used in previous studies when scaling these to the dimensions of our potato model (0.59e-8 mol/s for Thompson and Holbrook (2003) and 6.24e-8 mol/s for Hölttä et al. (2006). Our initial parameter settings resulted in a steady-state flow velocity in the base of the stem of 0.23 mm/s, which is in the same order of magnitude as the 0.34 mm/s measured in potato (Aliche et al., 2020; Prusova, 2016). Given that sieve tube radius data were taken from tomato rather than potato, we decreased sieve tube radius by 21.5% to 8.4e-6m to reproduce the measured potato sap flow velocity of 0.34 mm/s, equal to a transit time of 49 min.

In Figure 2, we show, starting from all zero initial conditions, the temporal dynamics (insets) and resulting steady-state gradients for the potato-specific model. Xylem pressure reached its steady state almost instantly, much faster than the phloem, that reached steady state in 3.9 hr. In steady state, the model generated sucrose concentrations of 1.69 M at the loading zone, 1.23 M at the middle of the stem, and 1.17 M at the start of the unloading zone, resulting in a sucrose gradient of 0.46 M/m_{length} between the end of the loading zone and the beginning of the unloading zone. While no experimental data on potato sucrose gradients in the phloem was available, sucrose concentrations range from 1.35 (Kehr, Hustiak, Walz, Willmitzer, & Fisahn, 1998) to 1.8 M (Pescod, Quick, & Douglas, 2007) in leaf phloem, indicating that our model lies well within the range of physiologically realistic values. As a further support of our model, a theoretical study by Jensen, Savage, and Holbrook (2013) demonstrated that the optimal concentration of sucrose for efficient transport is 1.01 M, close to our observed values. Additionally, they reported potato as the species with the highest phloem sucrose concentration in their review of 41 different species. Simulated steady-state turgor pressure in the middle of the stem was 3.8 MPa (closely matching the osmotic pressure of 4.1 MPa). Again, no data on potato phloem pressure were available, however pressure measurements in other plants range from 0.6 to 2.4 MPa (Fisher & Cash-Clark, 2000; Turgeon, 2010). In wheat (*Triticum aestivum*), in which the highest phloem pressure was measured, sucrose concentrations ranged from 0.25 (Hayashi & Chino, 1986) to 0.51 M (Fisher & Gifford, 1987). The steady-state pressure gradient generated by the model is 0.2Mpa/m, in the upper end of the range of experimentally observed pressure gradients (0.03–0.2Mpa/m; Hammel, 1968). Overall, the high hydrostatic pressure is in line with reports of steeper pressure gradients in herbaceous species and active loaders (Comtet, Jensen, Turgeon, Stroock, & Hosoi, 2017), and the higher sucrose concentration in crop species (Jensen et al., 2013).

Despite the high axial permeability in potato and the here observed high hydrostatic pressure, sap flow velocity did not exceed previously reported values (Hölttä et al., 2006; Thompson & Holbrook, 2003; Windt, Vergeldt, Jager, & As, 2006), as one may naively expected from combining these two factors. Instead, the high sucrose concentration resulted in high viscosity and hence a high transport resistance.

3.2 | Effect of SWEET-mediated efflux on transport characteristics

3.2.1 | Variation in SWEET v_{max}

We next set out to study the potential effects of StSWEET11-mediated sucrose efflux from the phloem on transport characteristics. We started

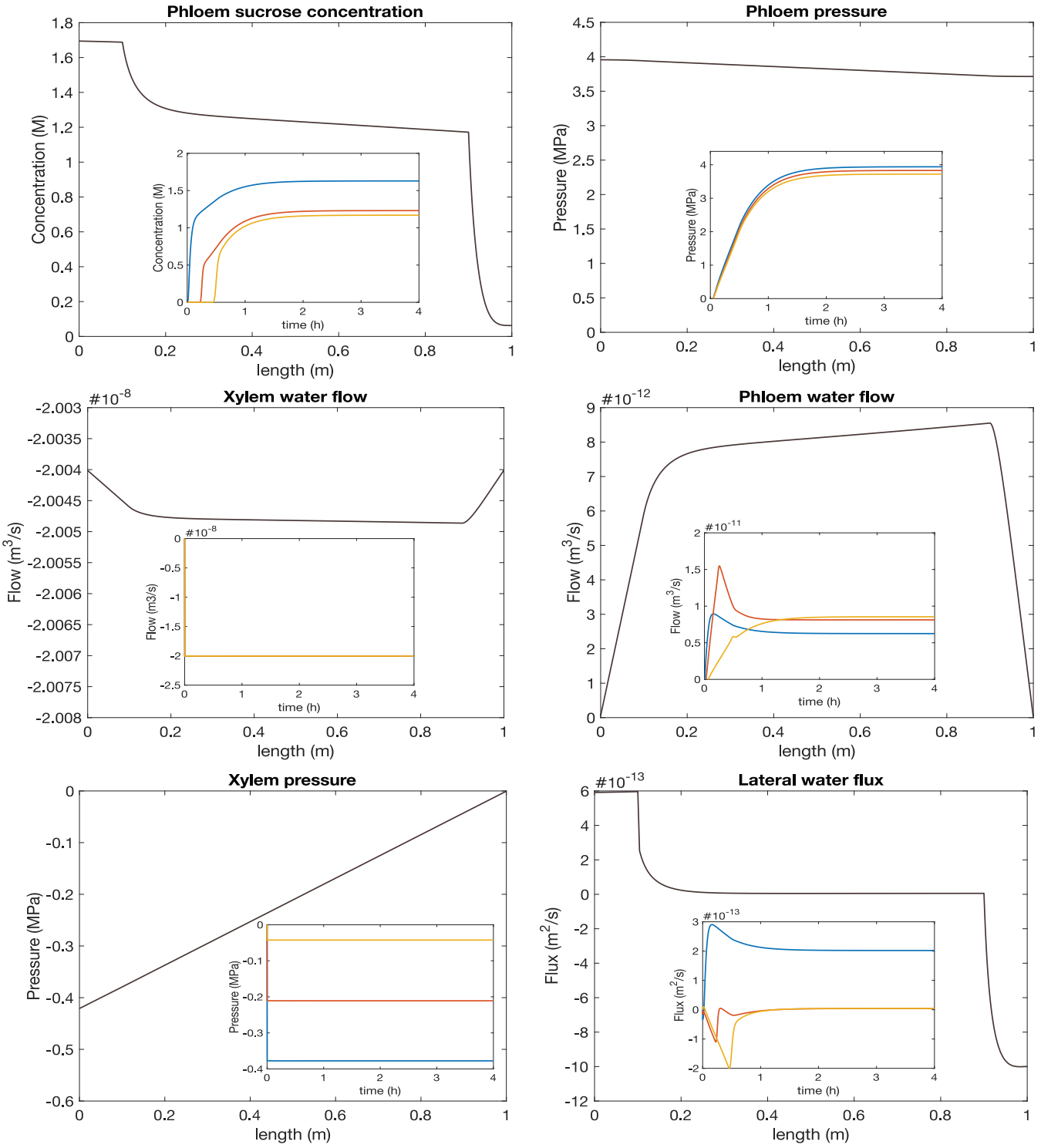

FIGURE 2 Gradients and dynamics of the baseline potato-specific model. The figures show the steady-state gradient over the length of the stem. The insets show the dynamics towards the steady state, where the blue line is the top element of the long-distance pathway, red the middle element, and yellow the bottom element [Colour figure can be viewed at wileyonlinelibrary.com]

with a worst-case scenario, in which, we ignored SUT-mediated retrieval from the apoplast, enabling us to explore the maximum effect on sucrose transport. SWEET-mediated sucrose transport has been experimentally quantified, but available data were restricted to non-potato SWEETs of different types (AtSWEET12, and VvSWEET7, Table S3). Experimental characterizations of SWEET transport are performed in heterologous expression systems, with expression levels and presence of co-factors likely different from the *in planta* conditions, suggesting that particularly measured v_{max} values should be treated with caution when extrapolating them to in *planta* transport. Indeed,

reported values ranged from 0.0012 (Chen et al., 2012) to 0.148 mol m^{-3} s^{-1} (Breia et al., 2020). Therefore, we first explored a broad range of v_{max} values (such that over the entire stem length it equals 0 to 100% of the total loading rate with a K_m of 10 mM) and quantified the effect and physiological significance on sucrose delivery. Simulated steady-state gradients for different export rates (Figures 3a, b, Figure S5) were qualitatively similar to the results of Minchin and Lacointe (2017). Below efflux rates of 5% of the baseline loading rate the effect of efflux along the stem was very small, and concentration and pressure gradients, as well as axial and lateral water flow decreased by less than 2%. At efflux rates of 10% the difference became more pronounced (Figure 3a, b, orange line) with concentration and pressure gradients decreasing 5%, this decrease increased linearly with increasing export rate. In this efflux-only scenario, delivery yield (Figure 1b) linearly decreased with efflux rate (Figure 3c). In line with the decreased sucrose concentrations resulting from efflux, we observed a substantial decrease in hydrostatic pressure levels, whereas the pressure gradient itself was much less affected. Finally, for efflux rates beyond 0.25× the baseline loading rate, the water flow velocity profile inverted, with higher flow rates at the top of the stem and decreasing along the stem, similarly to the results of Minchin and Lacointe (2017) (Figure 3b). Our broad exploration of efflux rates thus indicates that these rates must amount to a minimum of 5–10% of the solute loading rate to result in significant differences in transport characteristics and efficiency.

We then implemented the range of experimentally reported v_{max} values in our model (Figure 3a, b green, light blue, red lines; Figure 3c, orange dots). The lower bound AtSWEET12 transport rate resulted in a decrease in sucrose delivery of 0.2% compared to the baseline, no-

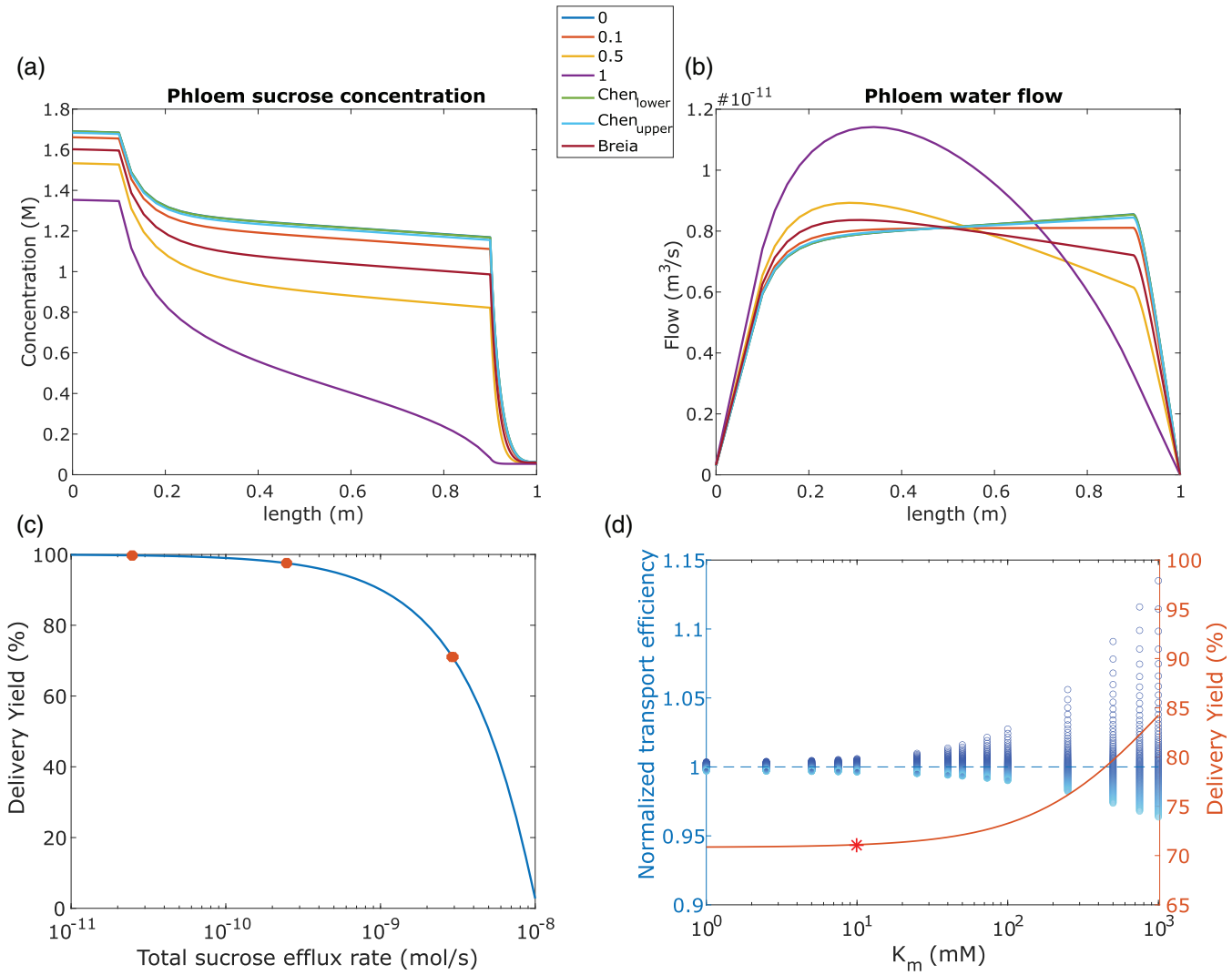

FIGURE 3 The effect of sucrose efflux. (a) Sucrose concentration gradient for different efflux rates (0, 0.1, 0.5 and 1 times baseline loading) and the SWEET rates from literature. (b) Water flow gradient for equal efflux rates. (c) Delivery yield along a range of efflux rates (v_{max}). The orange dots represent experimentally measured v_{max} values (Breia et al., 2020; Chen et al., 2012). (d) Effect of the affinity constant (K_m) on efflux. Dots represent transport efficiency along the stem normalized for mean efficiency per element, the colour gradient represents the location in the long-distance zone, with dark indication shootward and light more rootward position. The orange line represents the delivery yield and the red star represents the transport efficiency at the K_m (10 mM) used in all other simulations [Colour figure can be viewed at wileyonlinelibrary.com]

efflux model, whereas the reported upper rate resulted in a 2.4% decrease. Implementation of the VvSWEET7 transport rate resulted in a 28.9% decrease in sucrose delivery and strongly changed transport dynamics (Figure 3a, b, red line). Thus, only the transport rate reported for VvSWEET7 significantly affected sucrose transport. Transport rates of VvSWEET7 and AtSWEET12 may differ due to structural differences at protein level, but differences in experimental conditions in the heterologous expression system are likely to also have contributed significantly. Based on the observation that stem apoplastic sucrose concentration is 61% lowered for knockout of StSWEET11 and 278% increased for up-regulation of StSWEET11 (Abelenda et al., 2019), and StSWEET11 transport thus significantly affects stem sucrose transport, we stipulate that *in planta* StSWEET11 transport rates must lie in the range of or above the rate reported for the VvSWEET7 rather than those for AtSWEET12. Importantly, our estimates for SWEET transport rate values that significantly affect sucrose transport efficiency were done in efflux-only simulations, and hence represent a lower bound for the *in planta* situation in which also retrieval mechanisms operate.

3.2.2 | Variation in SWEET K_m

K_m values for VvSWEET7 and AtSWEET12 were found to lie between 10 and 73 mM (Table S3). It is noteworthy that typical potato phloem sap sucrose concentration exceeds 1 M (Kehr et al., 1998; Pescod et al., 2007), indicating that SWEET transporters typically operate at or near their maximum transport potential. Similar to the StSWEET11 v_{max}, we investigated the impact of different K_m values on sucrose transport characteristics, varying K_m values from 1 to 1,000 mM, while using the VvSWEET7 efflux rate. As expected, an increase in K_m decreased the effective efflux rate. A K_m increased from 10 to 75 mM decreased total efflux with 5.2%, whereas an increase to 500 mM decreased efflux with 39.1%. In contrast, a decrease to 1 mM, increased efflux by only 0.7%, due to the near saturation of SWEET transport already occurring at the default K_m of 10 mM (Figure 3d, orange line). For higher K_m values, we observed a large increase in the variance of element specific transport efficiency along the stem (Figure 3d, blue dots). At high K_m, as the concentration decreased along the stem, transport efficiency increased due to reduced saturation of the transporter, effectively decreasing efflux rate. However, even for a total efflux rate equal to the loading rate and low K_m values, not all sucrose was lost prior to arrival at the unloading zone. Counterintuitively, despite the K_m of 10 mM being up to 17 times lower than phloem sucrose concentrations, the decrease in sucrose concentration along the stem, still resulted in a small decrease in effective efflux-rate even for low K_m. In this simple efflux-only system, the saturating dynamics of the SWEET transporter already affects sucrose transport in a non-linear manner.

3.3 | Efflux-retrieval dynamics and SWEET-efflux mitigation

SUT-mediated sucrose retrieval from the apoplast is expected to significantly mitigate sucrose loss. As discussed above, the SWEET v_{max} values estimated to have a physiologically relevant effect in absence of retrieval represent a lower bound. To ensure physiological relevance upon incorporation of a retrieval mechanism, SWEET v_{max} values were doubled. Earlier theoretical work on the efflux-retrieval mechanism generated apoplast sucrose dynamics that were much slower than phloem transport (Minchin & Lacointe, 2017). Because of the slow apoplast timescale, this resulted in excessively long, physiologically unrealistic times to equilibrate (up to 10^4 hr), making them only suitable for studying steady-state dynamics. Here, we aim for our model to also be suitable to investigate transient sucrose transport dynamics.

3.3.1 | The effect of the apoplast volume

Minchin and Lacointe (2017) assumed that apoplast volume was 1,000 times larger than that of the phloem. This implies that for sucrose exchange between phloem and apoplast, a change in phloem concentration is accompanied by a 1,000-fold smaller change in apoplast concentration, and thus likely plays an important role in slow apoplast dynamics. Indeed, similar to their observations, we did find a linear relation between equilibration time and apoplast volume (Figure 4a, Blue line), decreasing from 3,031 hr for apoplast volumes of 1,000 times phloem volume to 30 hr for apoplast volumes of 10 times the phloem volume. For small apoplast volumes (<2× phloem volume), the equilibration time was not solely determined by apoplast volume and the linear relation no longer applied. Next, we estimated what would be a realistic phloem-apoplast ratio from available volume measurements. Measurements on potato leaves reported that 5% of leaf volume is composed of vasculature and 3% of apoplast (Leidreiter, Kruse, Heineke, Robinson, & Heldt, 1995). In absence of further data, we assume that, given the highly vascularized nature of plant leaves, these data represent and upper limit of the vascular volume fraction in the entire plant. Additionally, we assume that the apoplastic fraction is approximately constant in different potato plant organs. Further, we have a phloem volume of 0.0252 ml and a xylem volume of 0.42 ml in the model. From this, we derived that the total volume share of the phloem is 0.28%. From a 3% volume share for the total apoplastic compartment in the stem, we then arrive at the apoplastic volume being 3/0.28 = 10.7 times larger than the phloem volume. While this calculation was based on a series of assumptions, we expect this estimate to be in the correct order of magnitude. Thus, from here on, we continue the simulations with an apoplast volume of 10 times that of the phloem volume.

3.3.2 | The effect of apoplastic sucrose removal

Above, we show that for an apoplast volume of 10 times, the phloem volume equilibration time was 30.0 hr, as compared to the 3.9 hr for the model without apoplast retrieval and otherwise similar settings. Based on this, we expect that other factors may contribute to shortening equilibrium time as well. Apoplastic sucrose is taken up by

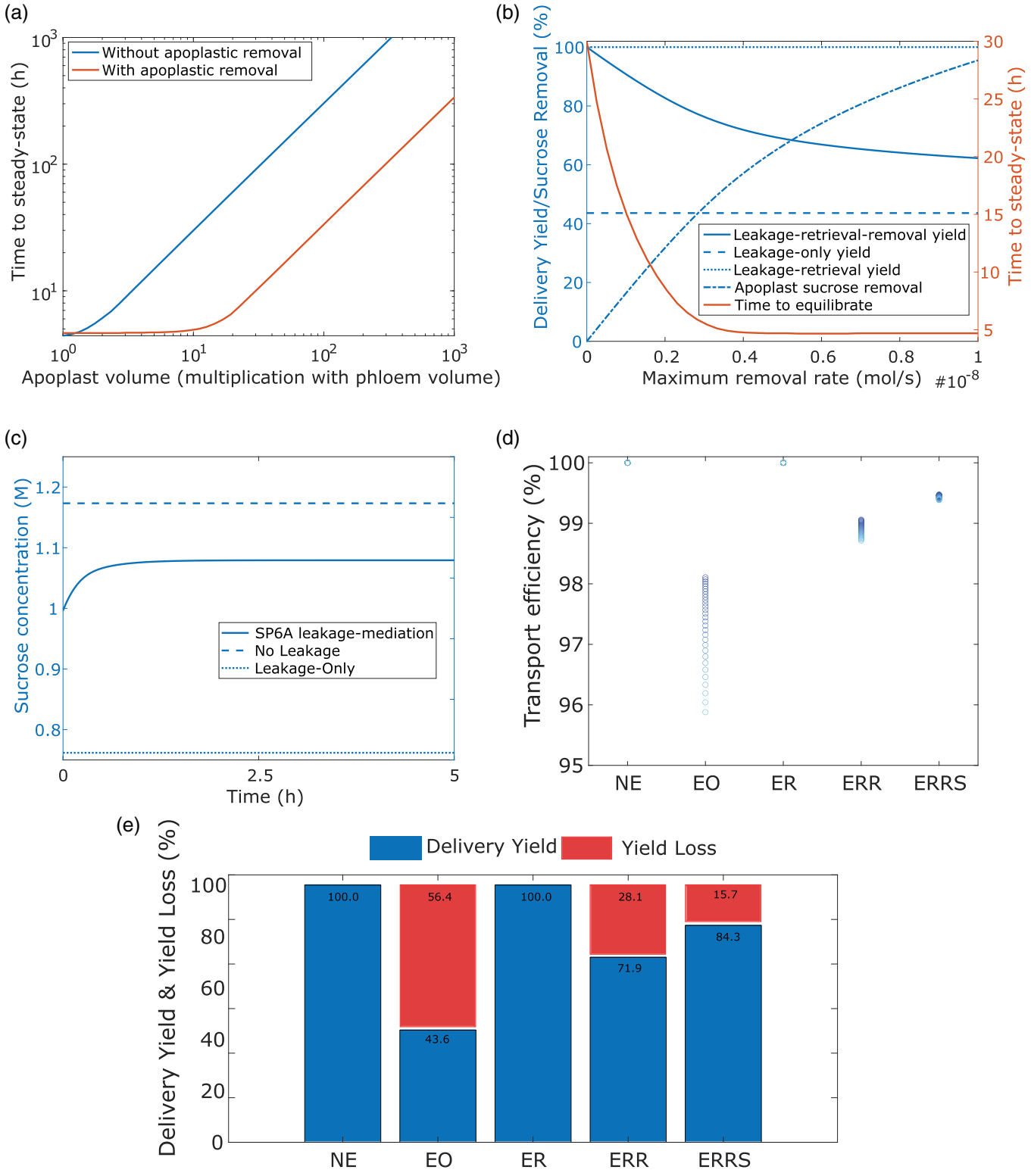

FIGURE 4 Efflux-retrieval dynamics and SWEET-efflux mitigation. (a) Time to reach steady state for varying apoplast volumes in a system with (0.4e-8 mol/s) and without apoplastic respiration and with a bidirectional SWEET and SUC transporters. (b) Delivery yield (percentage of maximum in absence of efflux), apoplast sucrose removal (percentage of sucrose influx) and time to steady state for varying removal rates in the apoplast. Apoplast sucrose removal is given as a percentage of sucrose influx in that specific compartment. (c) Sucrose concentration after the introduction of StSP6A-mediated efflux-decrease and no-efflux and efflux-only scenarios as comparison. (d) Transport efficiency per element for different efflux scenarios. The colour gradient represents the location in the long-distance zone, with dark indication shootward and light more rootward position. NE, No-Efflux; EO, Efflux-only; ER, Efflux-Retrieval; ERR, Efflux-Retrieval-Removal; ERRS, Efflux-Retrieval-Removal-StSP6A. (e) Delivery yield in the 24 h after reaching steady state for the same scenarios as in (d) [Colour figure can be viewed at wileyonlinelibrary.com]

neighbouring cells for their growth and maintenance as well as consumed by resident pathogens (Chen, 2014; Lemoine et al., 2013). These processes, which all contribute to irreversible loss of sucrose from the apoplast, we here named apoplastic sucrose removal. We hypothesized that incorporating these processes would reduce equilibration time and investigated this by varying the maximum rate of sucrose removal (R_{max}) between 0 and 1e-8 mol/s, using Michaelis–Menten kinetics with a constant $K_{m,R}$ of 5 mM. Without apoplastic sucrose removal, the apoplast sucrose concentration at the middle of the stem was 105.2 mM, which was significantly higher than the measured concentration in the potato stem apoplast of approximately 10 mM (Abelenda et al., 2019). Implementation of sucrose removal in the apoplast strongly decreased the sucrose concentration in the apoplast to 56.8 mM for an apoplast removal rate of 0.1e-8 mol/s and 11.8 mM for a removal rate of 0.4e-8 mol/s, the latter closely fitting the experimental data. In parallel with a decrease mostly in apoplast, but also phloem sucrose concentrations, higher sucrose removal rates indeed resulted in a strong decrease in equilibration times (Figure 4b, orange line). For the highest modelled sucrose removal rate, equilibration time was only slightly higher than for simulations without apoplast (4.7–3.9 hr). A similar linear dependence between equilibration time and apoplastic volume for absence and presence of sucrose removal (Figure 4a, orange line), yet this linear dependence occurred considerably above the apoplastic volume threshold. As a consequence, for a sufficiently high removal rate and 10 times higher apoplast than phloem volume, we stay outside the regime where apoplast volume determined equilibration times. Overall, inclusion of apoplastic sucrose removal representing sucrose consumption elsewhere, further improved the fit between simulated and measured apoplastic sucrose concentrations as well as decreased the time for simulations to equilibrate.

Including sucrose retrieval and removal also strongly improved delivery yield compared to the worst-case efflux-only (EO) case, with efflux-retrieval-removal (ERR) asymptotically approaching EO yield levels as removal rates increase (Figure 4b). This asymptotic decline of yield arises from the saturating Michaelis–Menten kinetics for apoplastic sucrose removal combined with the decrease in apoplast concentration sucrose concentration for high removal rates, causing the same increase in removal rates to have less and less effect on sucrose levels.

3.3.3 | The effect of the StSWEET11–StSP6A interaction

Fixing the v_{max} of the apoplastic sucrose removal rate at 0.4e-8 mol/s, we next set out to study the effect of StSP6A on equilibration times and transport characteristics. We started simulations from a steady state with fully operational SWEET sucrose-efflux and then decreased the SWEET v_{max} with 40% to simulate maximum StSP6A production. It took 2.8 hr to reach the new steady state (Figure 4c). Instead of the instantaneous onset of maximum StSP6A production as modelled here, *in planta* it takes 2–4 days in leaves and 4–8 days in tubers to reach maximum StSP6A (Navarro et al., 2011). This implies that the timing of physiological StSP6A effects is dominated by StSP6A production dynamics rather than long-distance transport equilibration dynamics.

We compared transport efficiency and variation therein, along the stem for the different scenarios considered (Figure 4d). We see that compared to the scenario of efflux retrieval and apoplast removal (ERR), StSP6A introduction (ERRS) caused enhanced average transport efficiency, as well as a reduced decrease in efficiency along the stem due to a smaller sucrose gradient in the phloem (Figure 4d). A similar increase in average efficiency and decrease in efficiency variation can be seen for the transition from EO to ERR.

Like transport efficiency, the delivery yield (Y) for LRRS increased relative to ERR simulations, as less efflux occurred due to decreased SWEET v_{max}. Y increased from 71.9% (ERR) to 84.3% (ERRS) of loaded sucrose. Reduction of StSWEET11-mediated efflux by StSP6A results in an increased sucrose retention in the phloem and thus a decrease in yield loss (100-Y) from 28.1 to 15.7% of loaded sucrose. Interestingly, a 40% decreased v_{max} thus resulted in a 44.1% decrease in yield loss. The StSP6A-mediated reduced efflux leads to lower apoplast sucrose levels, which due to the saturated dependence of sucrose removal on sucrose levels causes a more than linear decrease in apoplast sucrose removal. As a consequence, decrease in yield loss is larger than efflux reduction. Depending on the parameter values, especially removal K_m, the decrease in yield loss increases further after StSP6A introduction. Increasing the sucrose removal K_m to 10 mM, a yield loss decrease of 47.9% was obtained.

3.4 | Transgenic StSWEET11 phenotypes

Transgenic StSWEET11 plants had large deviations in apoplast sucrose concentrations (Table S4, Abelenda et al., 2019). We recreated the StSWEET11 knockdown (StSWEET11 RNAi), StSWEET11 over-expression (35S:StSWEET11), and StSWEET11/StSP6A over-expression (35S:StSWEET11/SUC2:StSP6A) genotypes to test whether changed SWEET-activity in our model could reproduce the measured apoplastic sucrose differences.

Transgenics were simulated by changing the SWEET v_{max} equally to the reported fold-change reported by Abelenda et al. (2019), being approximately doubled for over-expression and decreased 20-fold for knockdown. The combined over-expression was simulated by first increasing the v_{max} fivefold (mimicking the StSWEET11 over-expression) and subsequently decreasing this v_{max} by 95% (mimicking 100-fold StSP6A over-expression), as we expect that the StSP6A increase would strongly increase the binding of StSP6A to StSWEET11, blocking almost all transport activity. Simulated apoplast sucrose concentration changes compared with the measured concentration changes were lower in the knockdown (−99 to −61%) and higher in the over-expression line (+438–+278%), whereas the simulated concentration change in the combined StSWEET11/StSP6A line was close to the measured concentration (−92 to −89%) (Table S4). Our model is a simplification by necessity and does not incorporate

regulatory processes allowing for compensatory increases or decreases in other transporters, or efficiency of the SWEET transporter itself. In case of StSWEET11 over-expression the 35S promotor was used that leads to ubiquitous expression, leaving open the possibility that not all of the 20-fold increase in StSWEET11 levels in leaves occurs in the phloem.

We therefore investigated the fold-changes in expression levels required in our simulated mutants to reproduce experimental observations. In case of StSWEET11 knockout, applying a 2.5-fold rather than 20-fold reduction in SWEET v_{max} resulted in an apoplast concentration of 2.2 mM, close to the experimental observations, suggesting a substantial, but not complete, replacement by StSWEET11mediated efflux by other transporters in the case of StSWEET11 knockdown. Similarly, in case of StSWEET11 overexpression, a 1.5-fold rather than twofold increase in v_{max} resulted in a concentration of 34.9 mM, suggesting that indeed substantial overexpression is outside the phloem or that retrieval was increased in case of increased SWEET-activity.

4 | DISCUSSION

Tuber yield is not only dependent on assimilate production in source-leaves but also on long-distance transport and sink-strength. Recently, it was shown in heterologous expression experiments that the potato tuberigen StSP6A-mediated a 40% reduction of StSWEET11 sucrose-export activity (Abelenda et al., 2019). Unfortunately, the complex multi-feedback nature of plant sucrose transport combined with the likely presence of additional StSP6A-mediated changes make it hard to assess the physiological relevance of the StSP6A-SWEET interaction on tuber yield. To resolve this, we here developed a mechanistic mathematical model of long-distance phloem transport in potato incorporating SWEET/SUT-mediated sucrose transport to study the effect of the StWEET11–StSP6A interaction.

Mathematical models on water and sucrose transport have so far largely been restricted to large plants and trees. Therefore, as a first step, we here developed the first quantitative, mechanistic model for sucrose transport in agronomically highly relevant potato plants. The model reproduced experimentally measured sap sucrose concentrations and velocities well. Interestingly, our model indicated that high viscosity in the phloem was the major resistance factor in potato, in contrast to sieve-tube geometry reported in earlier work on larger plants (Stanfield, Schulte, Randolph, & Hacke, 2019; Thompson & Holbrook, 2003). This result is consistent with the higher sucrose concentration (Jensen et al., 2013), shorter stem-length, and higher flow velocity (Comtet et al., 2017; Windt et al., 2006) reported for herbaceous species, suggesting it might be a general property of small herbaceous crop species.

As a next step, we extended our model with SWEET sucrose transporters. Importantly, Abelenda and co-workers reported significant effects of StSWEET11 RNAi knockdown and overexpression on stem apoplast sucrose levels, supporting the physiological relevance of unblocked StSWEET11-mediated sucrose export in the stem (Abelenda et al., 2019). Importantly, SWEET transport rates were characterized in heterologous expression systems, resulting in highly variable reported maximum transport rates (Breia et al., 2020; Chen et al., 2012), with no data available for *in planta* transport rates. Using our model, we find that for SWEET mediated export to significantly affect sucrose transport characteristics, transport rates should lie in the upper range of the experimentally reported values. Importantly, these results were obtained in absence of simulated SUT-mediated sucrose retrieval, rendering this a lower boundary estimate and suggesting that *in planta* values should in fact lie at least a factor 1.5–2 higher. Our results thus underline that caution should be taken when interpreting transport rates obtained in heterologous expression experiments.

Surprisingly, we found that earlier studies that used explicit apoplastic volume and SUC-mediated sucrose retrieval, assumed very large apoplastic to phloem volume ratios (1,000:1) (Minchin & Lacointe, 2017). However, simple geometric considerations on potato stem diameter and the percentage of stem area occupied by phloem and xylem tissue indicate that this ratio cannot exceed 10.7:1. Importantly, we demonstrated that application of realistic apoplast to phloem volume ratios significantly reduces the long equilibration times these earlier models were suffering from. In addition, in earlier models, sucrose could only leave the apoplast through SUC-mediated re-uptake in the phloem. Therefore, after equilibration, SWEET-mediated sucrose loss equals SUC-mediated sucrose gain. Biologically, it seems logical to assume that sucrose efflux to the apoplast serves to supply surrounding stem tissue with energy, and hence that part of the sucrose efflux into the apoplast will be taken up and metabolized and thus no longer be available for re-uptake. Incorporating an apoplastic removal term to simulate this further decreased model equilibration time. Combined, these two adjustments ensure that the timescale of model dynamics are largely independent of whether an apoplast is explicitly simulated. We thus propose that our model is the first efflux-retrieval sucrose transport model resulting in biologically meaningful equilibration times.

Using the improved, potato-specific efflux-retrieval model, we studied the physiological significance of the StSP6A-mediated 40% efflux reduction. We found that after onset of StSP6A production, delivery yield increased over a physiologically relevant time-course of 3.5 hr. Furthermore, we demonstrate that for the deduced StSWEET11 transport rates used here, a reduction in StSWEET11-mediated efflux resulted in a significantly larger (10–20%) decrease in yield loss. This result not only supports the idea that StSP6A-mediated StSWEET11 blockage is physiologically relevant for potato yield but once more demonstrates how the feedback and non-linearities in plant sucrose transport necessitate mechanistic modelling to understand and predict the effects of imposed changes.

We hope and aim for the model developed in this study to serve as a valuable open-source tool for investigating yield improvement in agronomically relevant crop species. As our study illustrates, mathematical modelling is essential to highlight how, for example, plant type differences determine which factors dictate phloem sap flow. Thus, modelling can play an important role in determining the type of

optimization, photosynthesis, sink strength or long-distance transport that for a particular crop species and condition is likely to result in the largest yield increase. Our model is also intended as a starting point for the development of more sophisticated models. A first logical extension for future work would be to incorporate the distinct modes of symplastic and apoplastic unloading, necessary to investigate the tuberization switch and its potential dependence on the StSP6A-StSWEET11 interaction. Another important extension would be to explicitly include tuber growth and couple this to the transport model. While organ growth has been extensively modelled for swelling fruits such as tomato, kiwi, peach and grapes (Cieslak et al., 2016; Fishman & Génard, 1998; Hall, Minchin, Clearwater, & Génard, 2013; Zhu et al., 2019), tuber expansion arises through a combination of cell division and swelling, requiring more sophisticated organ growth modelling (Vreugdenhil, Chun, Jung, van Lammeren, & Ewing, 1999). To enable the investigation of resource competition between organs, as well as source-sink distance on sink resource uptake it will be necessary to replace the single, unbranched, source-sink architecture applied here with a more realistic plant architecture. The feasibility of this approach was recently demonstrated (Zhou et al., 2020). Finally, extension of the model with the regulatory networks controlling photosynthesis, plant architecture and the expression levels, patterns and activities of key factors such as StSP6A, SWEET and SUT would enable the incorporation of environmental factors impinging on these networks. Future model developments would greatly benefit from additional experimental data. As an example, detailed potato phloem morphology data and apoplast volume ratios could be obtained by a combined confocal and electron microscopy approach.

ACKNOWLEDGMENTS

This work was done in the framework of the MAMY project, with BH and SB funded by TTW (grant number 16889.2019C00026), jointly funded by MinLNV and the HIP consortium of companies.

CONFLICT OF INTEREST

The authors declare that there is no conflict of interest.

ORCID

Kirsten ten Tusscher https://orcid.org/0000-0002-1945-7858

REFERENCES

Abelenda, J. A., Bergonzi, S., Oortwijn, M., Sonnewald, S., Du, M., Visser, R. G. F., … Bachem, C. W. B. (2019). Source-sink regulation is mediated by interaction of an FT homolog with a SWEET protein in potato. *Current Biology*, *29*(7), 1178–1186. https://doi.org/10.1016/j.cub.2019.02.018

Aliche, E. B., Prusova-Bourke, A., Ruiz-Sanchez, M., Oortwijn, M., Gerkema, E., Van As, H., Visser, R. G. F., & van der Linden, C. G. (2020). Morphological and physiological responses of the potato stem transport tissues to dehydration stress. *Planta*, *251*(2), 45. https://doi.org/10.1007/s00425-019-03336-7

Aubry, E., Dinant, S., Vilaine, F., Bellini, C., & Le Hir, R. (2019). Lateral transport of organic and inorganic solutes. *Plants*, *8*(1). https://doi.org/10.3390/plants8010020

Bethke, P. C., Sabba, R., & Bussan, A. J. (2009). Tuber water and pressure potentials decrease and sucrose contents increase in response to moderate drought and heat stress. *American Journal of Potato Research*, *86*(6), 519–532. https://doi.org/10.1007/s12230-009-9109-8

Breia, R., Conde, A., Pimentel, D., Conde, C., Fortes, A. M., Granell, A., & Gerós, H. (2020). VvSWEET7 is a mono- and disaccharide transporter up-regulated in response to Botrytis cinerea infection in grape berries. *Frontiers in Plant Science*, *10*. https://doi.org/10.3389/fpls.2019.01753

Cabrita, P., Thorpe, M., & Huber, G. (2013). Hydrodynamics of steady state phloem transport with radial leakage of solute. *Frontiers in Plant Science*, *4*. https://doi.org/10.3389/fpls.2013.00531

Chen, L. Q. (2014). SWEET sugar transporters for phloem transport and pathogen nutrition. *New Phytologist*, *201*(4), 1150–1155. https://doi.org/10.1111/nph.12445

Chen, L.-Q., Qu, X.-Q., Hou, B.-H., Sosso, D., Osorio, S., Fernie, A. R., & Frommer, W. B. (2012). Sucrose efflux mediated by SWEET proteins as a key step for phloem transport. *Science*, *335*(6065), 207–211. https://doi.org/10.1126/science.1213351

Cieslak, M., Cheddadi, I., Boudon, F., Baldazzi, V., Génard, M., Godin, C., & Bertin, N. (2016). Integrating physiology and architecture in models of fruit expansion. *Frontiers in Plant Science*, *7*. https://doi.org/10.3389/fpls.2016.01739

Comtet, J., Jensen, K. H., Turgeon, R., Stroock, A. D., & Hosoi, A. E. (2017). Passive phloem loading and long-distance transport in a synthetic tree-on-a-chip. *Nature Plants*, *3*(4), 1–8. https://doi.org/10.1038/nplants.2017.32

De Schepper, V., & Steppe, K. (2010). Development and verification of a water and sugar transport model using measured stem diameter variations. *Journal of Experimental Botany*, *61*(8), 2083–2099. https://doi.org/10.1093/jxb/erq018

Driever, S. M., Simkin, A. J., Alotaibi, S., Fisk, S. J., Madgwick, P. J., Sparks, C. A., … Raines, C. A. (2017). Increased SBPase activity improves photosynthesis and grain yield in wheat grown in greenhouse conditions. *Philosophical Transactions of the Royal Society of London. Series B, Biological Sciences*, *372*(1730), 20160384. https://doi.org/10.1098/rstb.2016.0384

Duarte-Delgado, D., Ñústez-López, C., Narváez-Cuenca, C., Restrepo-Sánchez, L., Melo, S. E., Sarmiento, F., … Mosquera-Vásquez, T. (2016). Natural variation of sucrose, glucose and fructose contents in Colombian genotypes of *Solanum tuberosum* group Phureja at harvest. *Journal of the Science of Food and Agriculture*, *96*(12), 4288–4294. https://doi.org/10.1002/jsfa.7783

Fernie, A. R., Bachem, C. W. B., Helariutta, Y., Neuhaus, H. E., Prat, S., Ruan, Y.-L., … Sonnewald, U. (2020). Synchronization of developmental, molecular and metabolic aspects of source–sink interactions. *Nature Plants*, *6*(2), 55–66. https://doi.org/10.1038/s41477-020-0590-x

Fisher, D. B., & Cash-Clark, C. E. (2000). Gradients in water potential and turgor pressure along the translocation pathway during grain filling in normally watered and water-stressed wheat plants. *Plant Physiology*, *123*(1), 139–148. https://doi.org/10.1104/pp.123.1.139

Fisher, D. B., & Gifford, R. (1987). Accumulation and conversion of sugars by developing wheat grains VI. Gradients along the transport pathway from the peduncle to the endosperm cavity during grain filling. *Plant Physiology*, *82*, 1024–1030. https://doi.org/10.1104/pp.82.4.1024

Fishman, S., & Génard, M. (1998). A biophysical model of fruit growth: Simulation of seasonal and diurnal dynamics of mass. *Plant, Cell & Environment*, *21*(8), 739–752. https://doi.org/10.1046/j.1365-3040.1998.00322.x

Hafke, J. B., van Amerongen, J.-K., Kelling, F., Furch, A. C. U., Gaupels, F., & Bel, A. J. E. v. (2005). Thermodynamic battle for photosynthate acquisition between sieve tubes and adjoining parenchyma in transport phloem. *Plant Physiology*, *138*(3), 1527–1537. https://doi.org/10.1104/pp.104.058511

Hall, A. J., Minchin, P. E. H., Clearwater, M. J., & Génard, M. (2013). A biophysical model of kiwifruit (*Actinidia deliciosa*) berry development. *Journal of Experimental Botany*, *64*(18), 5473–5483. https://doi.org/10.1093/jxb/ert317

Hammel, H. T. (1968). Measurement of turgor pressure and its gradient in the phloem of oak. *Plant Physiology*, *43*(7), 1042–1048. https://doi.org/10.1104/pp.43.7.1042

Hayashi, H., & Chino, M. (1986). Collection of pure phloem sap from wheat and its chemical composition. *Plant and Cell Physiology*, *27*(7), 1387–1393. https://doi.org/10.1093/oxfordjournals.pcp.a077237

Hölttä, T., Mencuccini, M., & Nikinmaa, E. (2009). Linking phloem function to structure: Analysis with a coupled xylem–phloem transport model. *Journal of Theoretical Biology*, *259*(2), 325–337. https://doi.org/10.1016/j.jtbi.2009.03.039

Hölttä, T., Vesala, T., Sevanto, S., Perämäki, M., & Nikinmaa, E. (2006). Modeling xylem and phloem water flows in trees according to cohesion theory and Münch hypothesis. *Trees*, *20*(1), 67–78. https://doi.org/10.1007/s00468-005-0014-6

Irvine, J., & Grace, J. (1997). Continuous measurements of water tensions in the xylem of trees based on the elastic properties of wood. *Planta*, *202*(4), 455–461. https://doi.org/10.1007/s004250050149

Jensen, K. H., Savage, J. A., & Holbrook, N. M. (2013). Optimal concentration for sugar transport in plants. *Journal of the Royal Society Interface*, *10*(83), 20130055. https://doi.org/10.1098/rsif.2013.0055

Jonik, C., Sonnewald, U., Hajirezaei, M.-R., Flügge, U.-I., & Ludewig, F. (2012). Simultaneous boosting of source and sink capacities doubles tuber starch yield of potato plants. *Plant Biotechnology Journal*, *10*(9), 1088–1098. https://doi.org/10.1111/j.1467-7652.2012.00736.x

Kehr, J., Hustiak, F., Walz, C., Willmitzer, L., & Fisahn, J. (1998). Transgenic plants changed in carbon allocation pattern display a shift in diurnal growth pattern. *The Plant Journal*, *16*(4), 497–503. https://doi.org/10.1046/j.1365-313x.1998.00318.x

Lacointe, A., & Minchin, P. E. H. (2008). Modelling phloem and xylem transport within a complex architecture. *Functional Plant Biology*, *35*(10), 772–780. https://doi.org/10.1071/FP08085

Leggewie, G., Kolbe, A., Lemoine, R., Roessner, U., Lytovchenko, A., Zuther, E., … Fernie, A. R. (2003). Overexpression of the sucrose transporter SoSUT1 in potato results in alterations in leaf carbon partitioning and in tuber metabolism but has little impact on tuber morphology. *Planta*, *217*(1), 158–167. https://doi.org/10.1007/s00425-003-0975-x

Leidreiter, K., Kruse, A., Heineke, D., Robinson, D. G., & Heldt, H.-W. (1995). Subcellular volumes and metabolite concentrations in potato (*Solanum tuberosum* cv. Désirée) leaves. *Botanica Acta*, *108*(5), 439–444. https://doi.org/10.1111/j.1438-8677.1995.tb00518.x

Lemoine, R., La Camera, S., Atanassova, R., Dédaldéchamp, F., Allario, T., Pourtau, N., … Durand, M. (2013). Source-to-sink transport of sugar and regulation by environmental factors. *Frontiers in Plant Science*, *4*. https://doi.org/10.3389/fpls.2013.00272

Mammeri, Y., & Sellier, D. (2017). A surface model of nonlinear, non-steady-state phloem transport. Retrieved from https://hal.archives-ouvertes.fr/hal-01372758

Michel, B. E. (1972). Solute potentials of sucrose solutions. *Plant Physiology*, *50*(1), 196–198. https://doi.org/10.1104/pp.50.1.196

Minchin, P. E. H., & Lacointe, A. (2017). Consequences of phloem pathway unloading/reloading on equilibrium flows between source and sink: A modelling approach. *Functional Plant Biology*, *44*(5), 507–514. https://doi.org/10.1071/FP16354

Morison, K. R. (2002). Viscosity equations for sucrose solutions: Old and new 2002. *Proceedings of the 9th APCChE Congress and CHEMECA*.

Mullendore, D. L., Windt, C. W., Van As, H., & Knoblauch, M. (2010). Sieve tube geometry in relation to phloem flow. *The Plant Cell*, *22*(3), 579–593. https://doi.org/10.1105/tpc.109.070094

Navarro, C., Abelenda, J. A., Cruz-Oró, E., Cuéllar, C. A., Tamaki, S., Silva, J., … Prat, S. (2011). Control of flowering and storage organ formation in potato by FLOWERING LOCUS T. *Nature*, *478*(7367), 119–122. https://doi.org/10.1038/nature10431

Nobel, P. S. (2005). *Physicochemical and environmental plant physiology*, Cambridge, MA: Academic Press.

Nölke, G., Houdelet, M., Kreuzaler, F., Peterhänsel, C., & Schillberg, S. (2014). The expression of a recombinant glycolate dehydrogenase polyprotein in potato (*Solanum tuberosum*) plastids strongly enhances photosynthesis and tuber yield. *Plant Biotechnology Journal*, *12*(6), 734–742. https://doi.org/10.1111/pbi.12178

Pagliarani, C., Casolo, V., Beiragi, M. A., Cavalletto, S., Siciliano, I., Schubert, A., … Secchi, F. (2019). Priming xylem for stress recovery depends on coordinated activity of sugar metabolic pathways and changes in xylem sap pH. *Plant, Cell & Environment*, *42*(6), 1775–1787. https://doi.org/10.1111/pce.13533

Perämäki, M., Nikinmaa, E., Sevanto, S., Ilvesniemi, H., Siivola, E., Hari, P., & Vesala, T. (2001). Tree stem diameter variations and transpiration in Scots pine: An analysis using a dynamic sap flow model. *Tree Physiology*, *21*(12–13), 889–897. https://doi.org/10.1093/treephys/21.12-13.889

Pescod, K. V., Quick, W. P., & Douglas, A. E. (2007). Aphid responses to plants with genetically manipulated phloem nutrient levels. *Physiological Entomology*, *32*(3), 253–258. https://doi.org/10.1111/j.1365-3032.2007.00577.x

Pourazari, F., Andersson, M., & Weih, M. (2018). Altered tuber yield in genetically modified high-amylose and oil potato lines is associated with changed whole-plant nitrogen economy. *Frontiers in Plant Science*, *9*. https://doi.org/10.3389/fpls.2018.00342

Prusova, A. (2016). Light on phloem transport (an MRI approach). https://doi.org/10.18174/389397

Ross, H. A., & Davies, H. V. (1992). Sucrose metabolism in tubers of potato (*Solanum tuberosum* L.): Effects of sink removal and sucrose flux on sucrose-degrading enzymes. *Plant Physiology*, *98*(1), 287–293. https://doi.org/10.1104/pp.98.1.287

Schans, J., & Arntzen, F. K. (1991). Photosynthesis, transpiration and plant growth characters of different potato cultivars at various densities of *Globodera pallida*. *Netherlands Journal of Plant Pathology*, *97*(5), 297–310. https://doi.org/10.1007/BF01974225

Secchi, F., & Zwieniecki, M. A. (2016). Accumulation of sugars in the xylem apoplast observed under water stress conditions is controlled by xylem pH. *Plant, Cell & Environment*, *39*(11), 2350–2360. https://doi.org/10.1111/pce.12767

Sellier, D., & Mammeri, Y. (2019). Diurnal dynamics of phloem loading: Theoretical consequences for transport efficiency and flow characteristics. *Tree Physiology*, *39*(2), 300–311. https://doi.org/10.1093/treephys/tpz001

Sevanto, S., Hölttä, T., & Holbrook, N. M. (2011). Effects of the hydraulic coupling between xylem and phloem on diurnal phloem diameter variation. *Plant, Cell & Environment*, *34*(4), 690–703. https://doi.org/10.1111/j.1365-3040.2011.02275.x

Sibout, R., Plantegenet, S., & Hardtke, C. S. (2008). Flowering as a condition for xylem expansion in Arabidopsis hypocotyl and root. *Current Biology: CB*, *18*(6), 458–463 10.1016/j.cub.2008.02.070.

Stanfield, R. C., Schulte, P. J., Randolph, K. E., & Hacke, U. G. (2019). Computational models evaluating the impact of sieve plates and radial water exchange on phloem pressure gradients. *Plant, Cell & Environment*, *42*(1), 466–479. https://doi.org/10.1111/pce.13414

Thompson, M. V., & Holbrook, N. M. (2003). Application of a single-solute non-steady-state phloem model to the study of long-distance assimilate transport. *Journal of Theoretical Biology*, *220*(4), 419–455. https://doi.org/10.1006/jtbi.2003.3115

Turgeon, R. (2010). The puzzle of phloem pressure. *Plant Physiology*, *154*(2), 578–581. https://doi.org/10.1104/pp.110.161679

Van Bel, A. J. E. (2003). The phloem, a miracle of ingenuity. *Plant, Cell & Environment*, *26*(1), 125–149. https://doi.org/10.1046/j.1365-3040.2003.00963.x

Vos, J., & van der Putten, P. E. L. (1998). Effect of nitrogen supply on leaf growth, leaf nitrogen economy and photosynthetic capacity in potato. *Field Crops Research*, *59*(1), 63–72. https://doi.org/10.1016/S0378-4290(98)00107-5

Vreugdenhil, D., Chun, X. X., Jung, S., van Lammeren, A. A. M., & Ewing, E. E. (1999). Initial anatomical changes associated with tuber formation on single-node potato (*Solanum tuberosum* L.) cuttings: A re-evaluation. *Annals of Botany*, *84*(5), 675–680. https://doi.org/10.1006/anbo.1999.0950

Windt, C. W., Vergeldt, F. J., Jager, P. A. D., & As, H. V. (2006). MRI of long-distance water transport: A comparison of the phloem and xylem flow characteristics and dynamics in poplar, castor bean, tomato and tobacco. *Plant, Cell & Environment*, *29*(9), 1715–1729. https://doi.org/10.1111/j.1365-3040.2006.01544.x

Zeeman, S. C., Kossmann, J., & Smith, A. M. (2010). Starch: Its metabolism, evolution, and biotechnological modification in plants. *Annual Review of Plant Biology*, *61*, 209–234. https://doi.org/10.1146/annurev-arplant-042809-112301

Zheng, S.-L., Wang, L.-J., Wan, N.-X., Zhong, L., Zhou, S.-M., He, W., & Yuan, J.-C. (2016). Response of potato tuber number and spatial distribution to plant density in different growing seasons in Southwest China. *Frontiers in Plant Science*, *7*. https://doi.org/10.3389/fpls.2016.00365

Zhou, X.-R., Schnepf, A., Vanderborght, J., Leitner, D., Lacointe, A., Vereecken, H., & Lobet, G. (2020). CPlantBox, a whole-plant modelling framework for the simulation of water- and carbon-related processes. *In Silico Plants*, *2*(1), 1–19. https://doi.org/10.1093/insilicoplants/diaa001

Zhu, J., Génard, M., Poni, S., Gambetta, G. A., Vivin, P., Vercambre, G., … Dai, Z. (2019). Modelling grape growth in relation to whole-plant carbon and water fluxes. *Journal of Experimental Botany*, *70*(9), 2505–2521. https://doi.org/10.1093/jxb/ery367

SUPPORTING INFORMATION

Additional supporting information may be found online in the Supporting Information section at the end of this article.

How to cite this article: van den Herik B, Bergonzi S, Bachem CWB, ten Tusscher K. Modelling the physiological relevance of sucrose export repression by an Flowering Time homolog in the long-distance phloem of potato. *Plant Cell Environ*. 2021;44:792–806. https://doi.org/10.1111/pce.13977